

Low-Frequency Waves in the Plasma Environment Around the Shuttle

Boris V. Vayner* and Dale C. Ferguson†
NASA Lewis Research Center, Cleveland, Ohio 44135

As a part of the Solar Array Module Plasma Interaction Experiment program, the Langmuir probe was employed to measure plasma characteristics during the flight of STS-62. The entire data set could be divided into two parts: i) low-frequency sweeps to determine voltage-current characteristics and to find the electron temperature and number density and ii) high-frequency turbulence data caused by electrostatic noise around the Shuttle. Broadband noise was observed at 250–20,000-Hz frequencies. Measurements were performed in RAM conditions; thus it seems reasonable to believe that the influence of spacecraft operations on plasma parameters was minimized. It is shown that ion acoustic waves were observed, and two kinds of instabilities are suggested to explain the origin of these waves. According to the purposes of the experiment, samples of solar cells were placed in the cargo bay of the Shuttle, and high negative bias voltages were applied to them to initiate arcing between these cells and the surrounding plasma. The arcing onset was registered by special counters, and data were obtained that included the amplitudes of current, duration of each arc, and the number of arcs per one experiment. The data were analyzed for two different situations: with arcing and without arcing. Electrostatic noise spectra for both situations were obtained, and strong correlations between the number of arcs and the intensity of noise were established.

Nomenclature

B	= magnetic field strength, Gs
C	= capacitance of the Shuttle, F
$D(f)$	= observed spectrum, V/Hz
E, E	= electrical field strength, V/m
F_i	= ion gyrofrequency, Hz
f	= frequency of plasma density fluctuations, Hz
f_{LH}	= lower hybrid resonance frequency, Hz
I, i	= Langmuir probe (LP) current, A
I_m	= arc peak current, A
k	= wave vector, m^{-1}
k_B	= Boltzmann constant, J/K
L	= spacecraft dimension, m
l	= mean free path, m
N_{arc}	= number of arcs per one experiment
n_e	= electron number density, m^{-3}
n_g	= number density of neutral molecules, m^{-3}
n_i	= ion number density, m^{-3}
$n(XX)$	= number density of species XX, m^{-3}
p	= neutral gas pressure, Pa
R	= distance from spacecraft surface, m
T_e	= electron temperature, eV
T_g	= initial water vapor temperature, K
T_i	= ion temperature, K
t	= time, s
U	= LP output voltage, V
V	= LP bias voltage, V
V_D	= plasma drift velocity, m/s
V_s	= spacecraft velocity, m/s
V_T	= molecule thermal speed, m/s
W_s	= ion acoustic waver (IAW) phase speed, m/s
α	= angle between the wave vector k and the relative velocity V_r
γ	= increment of instability, s^{-1}
Δ	= duration of an arc, s

Θ	= angle between the Earth magnetic field and the spacecraft velocity
Λ	= Debye length, m
λ	= IAW wavelength, m
σ	= molecular cross section, m^2
τ_{exp}	= duration of individual experiment with arcing, s
τ_{dwell}	= duration of one dwell, s
φ	= angle between the wave vector k and the Earth's magnetic field B
$\omega_{1,2}$	= ion plasma frequencies, Hz

Introduction

DURING Space Shuttle flight STS-62, broadband electrostatic noise was observed at 250–20,000-Hz frequencies. The measurements were performed in RAM conditions by the Langmuir probe (LP) flown as a part of the Solar Array Module Plasma Interaction-Experiment (SAMPIE) package.¹ The noise has almost a flat spectrum with a sharp decline near the lower hybrid resonance frequency f_{LH} , and the intensities range from 0.1 to 5 mV/m (Ref. 2). Such noise was observed in RAM conditions more than ten years ago,³ but there is not yet a satisfactory explanation for the mechanism of generation. An investigation of plasma wave turbulence within a wide range of frequencies (from a few hertz to 200 kHz) was done by using the Plasma Diagnostic Package (PDP)

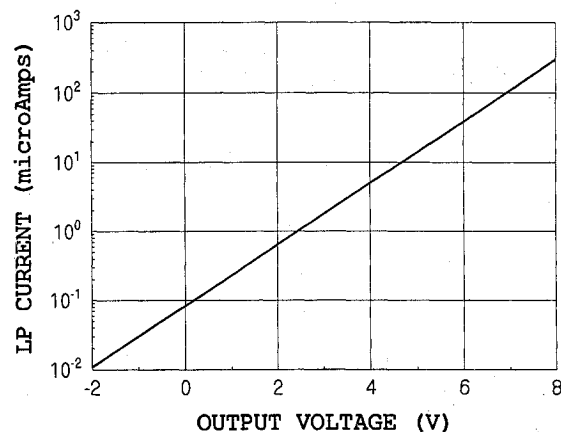


Fig. 1 Voltage-current characteristic of the logarithmic amplifier.

Received Aug. 4, 1995; revision received Oct. 30, 1995; accepted for publication Nov. 1, 1995. Copyright © 1996 by the American Institute of Aeronautics and Astronautics, Inc. No copyright is asserted in the United States under Title 17, U.S. Code. The U.S. Government has a royalty-free license to exercise all rights under the copyright claimed herein for Governmental purposes. All other rights are reserved by the copyright owner.

*National Research Council–NASA Research Associate. Member AIAA.

†Chief, Space Environment Effects Branch.

during the SL-2 and STS-3 flights.^{4,5} It was established that the noise is electrostatic; the highest intensities occurred in the region downstream of the spacecraft, particularly near regions with a steep gradient in plasma pressure; and the intensities increased considerably after water dumps.⁶ Two different processes were considered in attempting to understand the generation (instability) of the plasma turbulence caused by a water release: the drift instability and the Ott-Farley instability caused by the ring distribution of the water ions. Model computations of the ion distribution function confirm the idea that this function is non-Maxwellian.⁷ Moreover, the so-called ring distribution was measured directly, and one may believe that the electrostatic broadband noise observed in the wake of the shuttle can be explained theoretically by that mechanism.⁸ However,

an additional analysis of the electrostatic noise generation mechanism is needed because there are essential differences in plasma parameters between the SAMPIE and PDP experiments—all of the SAMPIE measurements of electrostatic noise [high-frequency turbulence (HFT) dwells] were performed in RAM conditions in the nearest vicinity of the Shuttle. The SAMPIE LP used a 5-cm-diam spherical sensor mounted on a fixed boom approximately 100 cm from the surface of the Shuttle,^{9,10} and fluctuations of electric current were measured by using a logarithmic amplifier with the current-voltage (I-V) characteristic shown in Fig. 1.¹¹ Each dwell lasted for 4 ms, and experimental data were represented in digital form: 80 measurements of current at 50- μ s intervals.

Spectra of the fluctuations were computed by using the fast Fourier transform procedure; thus we are able to study the plasma

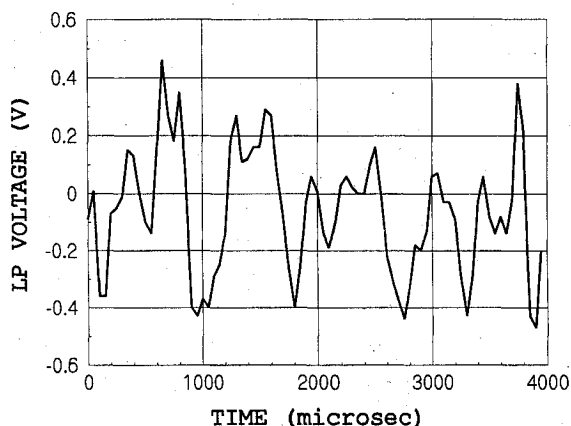


Fig. 2a HFT dwell recorded during the experiment E.44-2/01. MET 7/15:43, electron number density $5.4 \times 10^5 \text{ cm}^{-3}$, electron temperature 0.12 eV, and neutral gas pressure 2.27 μ torr.

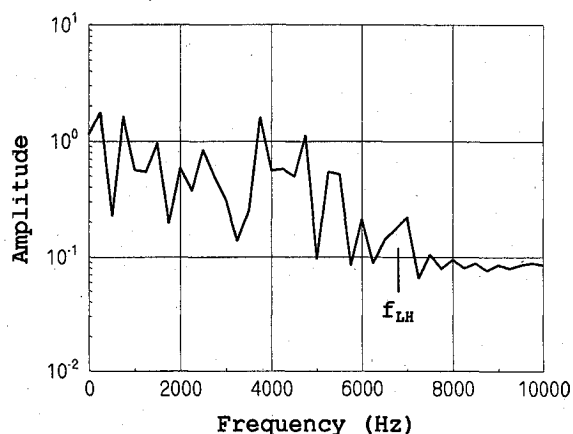


Fig. 3b Spectrum of the signal shown in Fig. 3a. $B = 0.46$ Gs and $\Theta = 80$ deg.

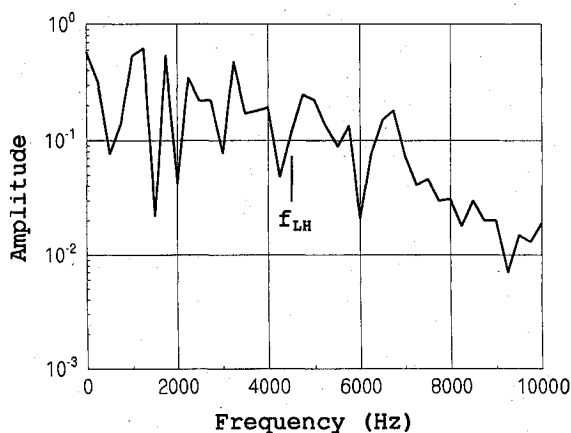


Fig. 2b Spectrum of signal shown above. Magnetic field strength $B = 0.25$ Gs, and angle between B and the velocity of shuttle $\Theta = -66.4$ deg.

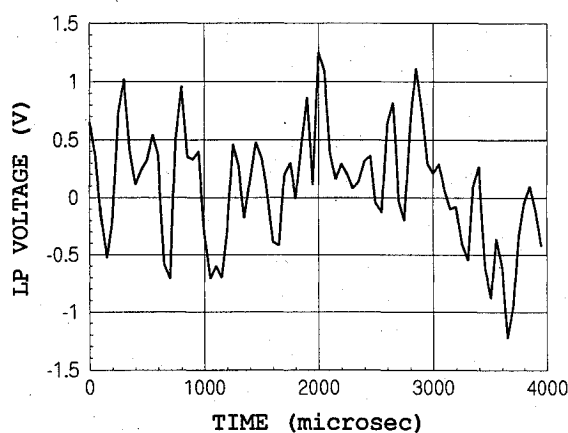


Fig. 4a Experiment E.48-2/01. MET 7/22:54, $n_e = 6 \times 10^5 \text{ cm}^{-3}$, $T_e = 0.1$ eV, and $p = 1.86 \mu$ torr.

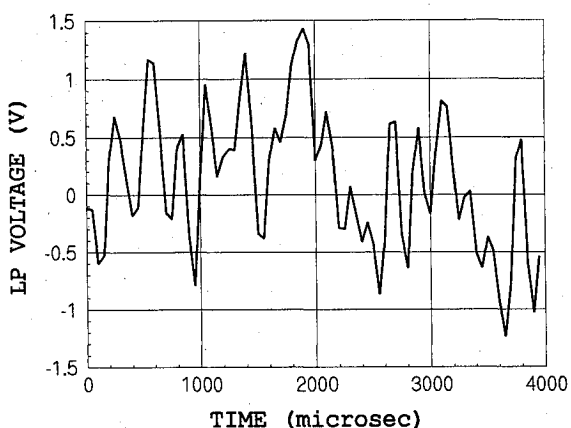


Fig. 3a Experiment E.62-2/03. MET 7/23:40, $n_e = 4.7 \times 10^5 \text{ cm}^{-3}$, $T_e = 0.17$ eV, and $p = 2.1 \mu$ torr.

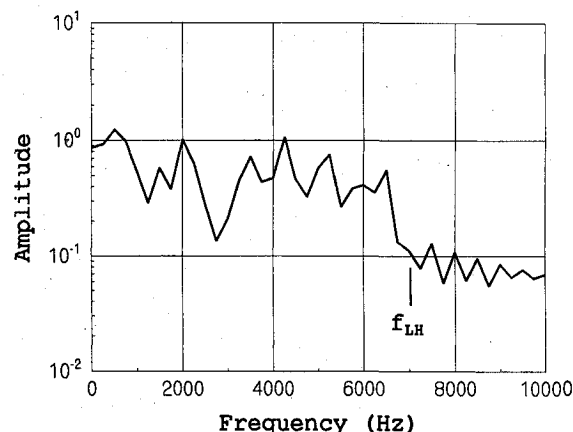


Fig. 4b Spectrum of the signal shown in Fig. 4a. $B = 0.52$ Gs and $\Theta = 90$ deg.

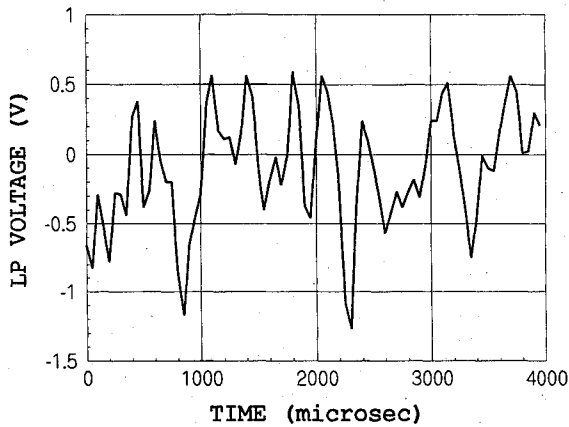


Fig. 5a Experiment 62_2/02. MET 7/23:39, $n_e = 3.8 \times 10^5 \text{ cm}^{-3}$, $T_e = 0.17 \text{ eV}$, and $p = 2.2 \mu\text{torr}$. All parameters are almost the same as in Fig. 3, but the amplitude of fluctuations is about five times less.

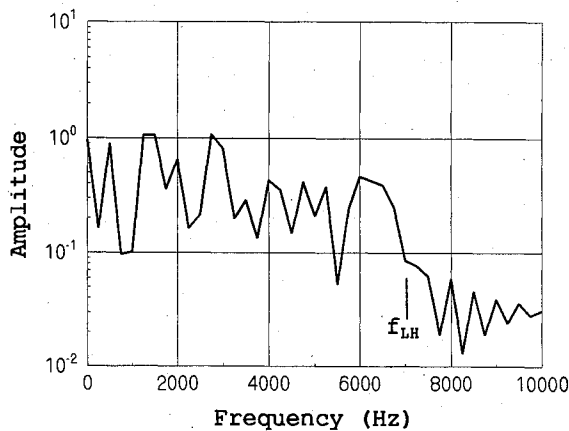


Fig. 5b Spectrum demonstrating a very sharp decline for frequencies $f \geq f_{\text{LH}}$.

turbulence within the narrow frequency interval $\Delta f = 250\text{--}10,000 \text{ Hz}$. Note that there is a likeness between spectra obtained by PDP and SAMPIE—they are relatively flat up to f_{LH} . On the other hand, we did not find any local peaks at frequencies $f \geq f_{\text{LH}}$. That could be considered as a difference between our results and PDP measurements.⁵ According to the purposes of the SAMPIE, the samples of solar cells were placed in the cargo bay of the shuttle, and high negative bias voltages were applied to them to initiate arcing between these cells and the surrounding plasma. It was shown that arcing influences the parameters of the electrostatic noise,² and we discuss this topic in the last section of this paper.

Observations

Three examples of HFT dwells with their spectra are shown in Figs. 2–4. The background plasma parameters (electron number density and temperature) were obtained by using the I–V characteristic of the LP.¹⁰ As can be seen, there are no essential differences among these graphs besides the amplitudes of the fluctuations: the amplitude of the current reaches $i_{\text{max}} \approx 0.1 \mu\text{A}$ for the dwell shown in Fig. 2, and the amplitudes are substantially higher for dwells shown in Figs. 3 and 4 ($i_{\text{max}} \approx 0.4 \mu\text{A}$). But if we take into account the difference in electron number densities for these three dwells, we may conclude that the level of fluctuations $\delta n_e/n_e$ is five times higher for the last dwell (Fig. 4).

All spectra demonstrate a sharp cutoff for frequencies $f \geq f_{\text{LH}}$. This fact could be considered an argument in favor of the ion acoustic waves (IAW) hypothesis because such kind of waves can be excited within the frequency range $F_i < f < f_{\text{LH}}$ if the electron temperature T_e is much greater than the ion temperature T_i that is valid for all of our HFT data. An HFT dwell that was recorded 1 min before the dwell shown in Fig. 3 demonstrates almost the same signal shape and spectrum, but the amplitude of fluctuations is about five times less (Fig. 5).

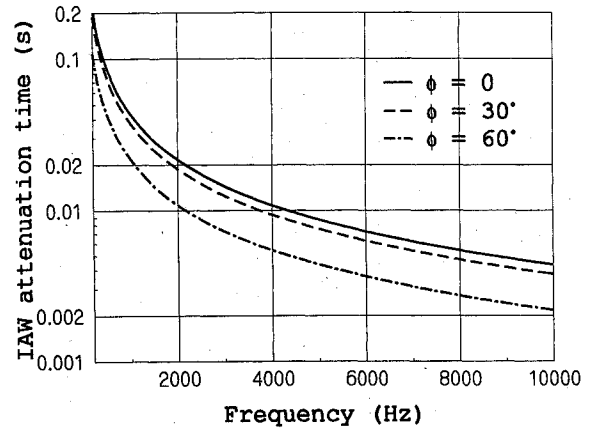


Fig. 6 IAW attenuation time vs frequency for three magnitudes of angle between the Earth's magnetic field and the wave vector (ϕ) ($T_e/T_i = 15$).

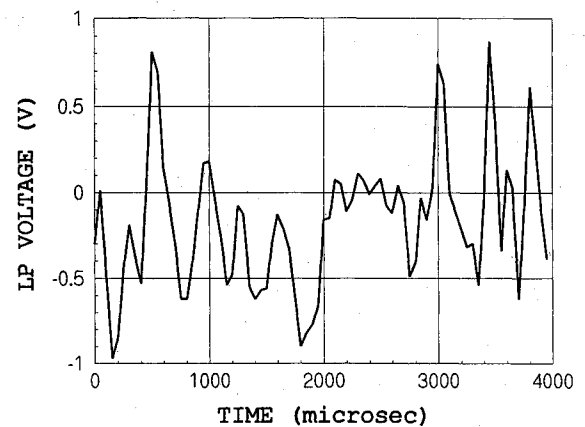


Fig. 7a Experiment E_46-1/01. MET 7/15:57, $n_e = 4.3 \times 10^4 \text{ cm}^{-3}$, $T_e = 0.14 \text{ eV}$, and $p = 1.85 \mu\text{torr}$.

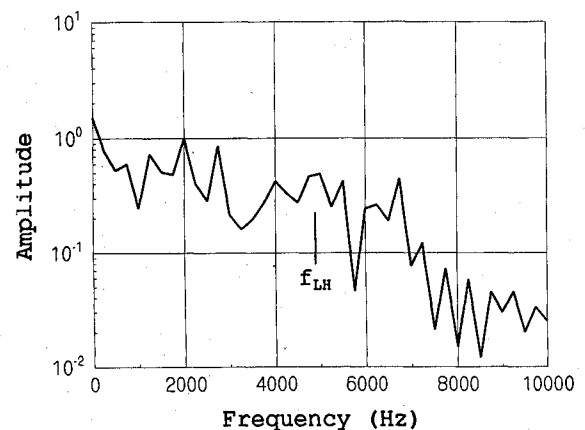


Fig. 7b Spectrum of the signal shown in Fig. 7a. $B = 0.33 \text{ Gs}$ and $\Theta = 74 \text{ deg}$.

One minute (60 s) is not a natural time scale for IAW because the calculations of the attenuation rate and instability increment for such waves show very short time intervals ($\tau = 3\text{--}100 \text{ ms}$) (Fig. 6).¹² The duration of one dwell ($\tau_D = 4 \text{ ms}$) is not long enough to observe any regular trend in amplitudes, although one could believe that the decrease of the amplitude for a time interval $t > 2 \text{ ms}$ is caused by real attenuation (Figs. 3 and 4). Some measurements were done in a plasma with a relatively low electron number density (Fig. 7). Here, the pressure of neutral gas is about 20% less than for the dwells shown above, but, surprisingly, the level of fluctuations is almost one order of magnitude higher. There are no essential differences in spectra between this dwell and other dwells.

For very low electron number density and low pressure of the neutral gas, only the instrument noise was registered. The origin and the characteristics of the observed electrostatic fluctuations must be explained by theory. We interpret these fluctuations in terms of IAW traveling in a weakly ionized plasma layer surrounding the Shuttle.

Interpretation

The Shuttle is surrounded by a gas cloud caused by many different processes accompanying spacecraft operations: outgassing of surfaces, leakage from valves, thrusters firing, etc.⁷ Molecules of the gas are moving at the thermal speed in the rest frame of the Shuttle, and ionospheric ions and neutral atoms can be considered an inflow with an average speed $V_s = 7.8$ km/s. If we suggest that the cloud is formed mainly from water vapor with an initial temperature $T_s \leq 300$ K, we may determine the number density of water molecules from measurements¹ of the gas pressure near the Shuttle:

$$n(\text{H}_2\text{O}) = \frac{p}{k_B T} = 6.4 \cdot 10^{10} \left(\frac{p}{2 \mu\text{torr}} \right) \left(\frac{T}{300 \text{ K}} \right)^{-1} \text{ cm}^{-3} \quad (1)$$

This value of the number density is a few times more than the number density of the ambient atmospheric gas at flight altitudes (220–310 km). According to direct computations, the water vapor densities at distances about 50 m from the Shuttle can be as large as $n(\text{H}_2\text{O}) = 2 \times 10^9 \text{ cm}^{-3}$, and this value reaches $4 \times 10^{10} \text{ cm}^{-3}$ in close to the spacecraft surface.⁷ Note that water molecules outgassed from the shuttle were directly observed during the flight of STS-39. According to IR emission data, the column density of water molecules was equal to $5 \times 10^{16} - 3 \times 10^{17} \text{ m}^{-2}$ (Refs. 13 and 14), and these measurements allow us to calculate the number density $n(\text{H}_2\text{O}) = 2 \times 10^{10} - 10^{11} \text{ cm}^{-3}$. Now, we can estimate the mean free path for a water molecule. The thermal speed is equal to

$$V_T = \left(\frac{2k_B T}{m(\text{H}_2\text{O})} \right)^{\frac{1}{2}} = 5.3 \cdot 10^4 \left(\frac{T}{300 \text{ K}} \right)^{\frac{1}{2}} \frac{\text{cm}}{\text{s}} \quad (2)$$

If we adopt as the cross section for molecular collisions $\sigma = 2 \times 10^{-15} \text{ cm}^2$ (Ref. 15) and the number density of the neutral gas $n_g \approx 10^{10} \text{ cm}^{-3}$, we will get a rough estimation for the mean free path

$$l = 1/(\sigma \cdot n_g) = 5 \times 10^4 \text{ cm} = 0.5 \text{ km} \quad (3)$$

which is much greater than the linear dimension of the spacecraft ($L \sim 10$ m). The time interval between two collisions is equal to

$$\tau = l/V_T = 1(T/300 \text{ K})^{-\frac{1}{2}} \text{ s} \quad (4)$$

These estimates allow us to write the radial dependence of the water molecule number density in the simple form⁷

$$n(\text{H}_2\text{O}) = n_0 [L/(L+R)]^2 \exp[-(R-L)/l] \quad (5)$$

Measurements of the electron temperature in the vicinity of the Shuttle are in the range $T_e = (0.1 - 0.3) \text{ eV}$.¹⁰ For IAW, the phase velocity is equal to

$$W_s = \left(\frac{k_B T_e}{m_i} \right)^{\frac{1}{2}} = 7.3 \times 10^4 \left(\frac{T_e}{0.1 \text{ eV}} \right)^{\frac{1}{2}} \frac{\text{cm}}{\text{s}} \quad (6)$$

According to the dispersion relation for IAW, the wavelength can be calculated as

$$\lambda = \frac{W_s}{f} = 73 \left(\frac{f}{1 \text{ kHz}} \right)^{-1} \left(\frac{T_e}{0.1 \text{ eV}} \right)^{\frac{1}{2}} \text{ cm} \quad (7)$$

where f is a frequency of fluctuations measured in the rest frame of the plasma.

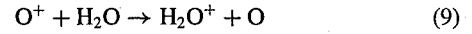
Thus, within the framework of the IAW hypothesis the wavelength of fluctuations is less than $3(T_e/0.1 \text{ eV})^{1/2} \text{ m}$ for the whole range of the observed frequencies. This means that we may consider the gas

layer surrounding the Shuttle as slightly nonhomogeneous because of the following inequalities:

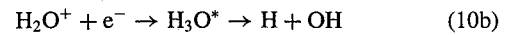
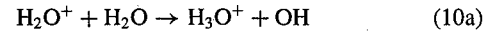
$$S_{LP} \leq \lambda_{\max} \ll L \ll l \quad (8)$$

In the relations (8), S_{LP} is the distance of the LP from the spacecraft surface.

Neutral water molecules that are ejected from the Shuttle surfaces will be ionized by an electrical charge exchange with ions O^+ having the flow velocity $V_0 = -7.8 \text{ km/s}$ and temperature $T_+ \leq 1000 \text{ K}$:



Three more reactions should be added to the reaction (9) to write the complete chain of reactions:



The kinetic equations for the reactions (9) and (10) were solved by using reaction rates tabulated in the work of Paterson and Frank.⁷ For particular case $n(\text{O}^+) = 2 \times 10^5 \text{ cm}^{-3}$, $n(\text{H}_2\text{O}) = 6 \times 10^{10} \text{ cm}^{-3}$, and $n_e = n(\text{O}^+) + n(\text{H}_2\text{O}^+) + n(\text{H}_3\text{O}^+)$, we obtain the ratio

$$x = \frac{n(\text{H}_2\text{O}^+)}{n(\text{H}_2\text{O})} = 3.9 \times 10^{-6} \quad (11)$$

As a result, the plasma comoving the Shuttle can be characterized by an ion number density as large as $(2-3) \times 10^5 \text{ cm}^{-3}$. In the rest frame of the shuttle, these ions are under the influence of a magnetic field \mathbf{B} and an induced electric field \mathbf{E} that is perpendicular to both vectors \mathbf{V}_s and \mathbf{B} ; and the electric field strength is equal to

$$\mathbf{E} = \mathbf{V}_s \mathbf{B} \sin \Theta = 0.23 \left(\frac{\mathbf{B}}{0.3 \text{ Gs}} \right) \sin \Theta \frac{\mathbf{V}}{\text{m}} \quad (12)$$

It is well known that electrically charged particles will drift with speed $\mathbf{V}_D = \mathbf{V}_s \sin \Theta$ in a direction that is perpendicular to both electric and magnetic fields. The angle between the Shuttle velocity and the magnetic field varied from $\Theta = -65$ to 90 deg during the experiments that are considered in this paper. This means that the projection of drift velocity directed to the surface of the shuttle V_{\perp} was always greater than the projection along the surface V_{\parallel} :

$$V_{\perp}/V_{\parallel} = |\tan \Theta| > 1 \quad (13)$$

We can conclude that there were two streams of ions with relative velocity

$$\mathbf{V}_r = -\mathbf{V}_s - \mathbf{V}_D \quad (14)$$

Thus it is possible to use the dispersion equation for IAW that may be written in the following form¹⁶:

$$1 + \frac{1}{k^2 \Lambda_1^2} + \frac{1}{k^2 \Lambda_2^2} - \left(\frac{\omega_1}{\omega} \right)^2 - \frac{\omega_2^2}{(\omega - k \cdot \mathbf{V}_r \cdot \cos \alpha)^2} = 0 \quad (15)$$

where

$$\Lambda = \left(\frac{k_B T_e}{4\pi \cdot e^2 n_e} \right)^{\frac{1}{2}}$$

The fourth-order equation (15) has complex roots (instability) if the following inequality can be fulfilled:

$$V_r^2 \cos^2 \alpha < W_s^2 \frac{\left(\omega_1^{\frac{1}{2}} + \omega_2^{\frac{1}{2}} \right)^3}{\omega_1 + \omega_2} \quad (16)$$

To obtain the inequality (16) we suggest $T_{e1} = T_{e2}$, and we take into account that the masses of oxygen and water ions are almost equal to each other.

For the simplest example $\omega_1 = \omega_2$, the condition of instability (16) can be written in the form

$$|\cos \alpha| < 2(W_s/V) \quad (17)$$

where $V = V_s \cos \theta$.

It is seen from expression (17) that the cone of instability is wide for $\Theta \approx 90$ deg. But the dispersion relation does not have complex roots when $\Theta = 90$ deg. In that case, the drift velocity is equal to the Space Shuttle speed exactly, and there is no relative motion of the two kinds of ions; thus the two-stream instability does not work when the spacecraft velocity is perpendicular to the Earth's magnetic field.

Now we can consider some specific experiments. For example, the angle between vectors V_s and B is equal to $\Theta = -66.4$ deg (Fig. 2). It is easy to calculate the IAW phase speed $W_s = 8 \times 10^4$ cm/s and $|\cos \alpha| < 0.5$. The complex frequency (the growing mode only) can be determined from Eq. (15):

$$\begin{aligned} \omega/kW_s &= 0.5 + i \times 0.34 & (\cos \alpha = 0.25) \\ \omega/kW_s &= 0.9 + i \times 0.24 & (\cos \alpha = 0.45) \end{aligned} \quad (18)$$

For different ion number densities $\omega_1/\omega_2 = 2$ we obtain almost the same result:

$$\omega/kW_s = 0.6 + i \times 0.33 \quad (\cos \alpha = 0.25) \quad (19)$$

During experiment E_62-2/03 the electron temperature was substantially higher (Fig. 3). The IAW speed was equal to $W_s = 9.5 \times 10^4$ cm/s, and the relative velocity of the ion streams was equal to $V = 1.36 \times 10^5$ cm/s. It is seen that for this particular experiment the beam velocity is almost equal (a little higher) to the IAW phase velocity. Such a condition is optimal for energy transfer from flux kinetic energy to fluctuations, and the rate of instability is high for all the magnitudes of angle between wave vector and stream velocity [see Eq. (17)]. This result depends on the relation between ion number densities only weakly:

$$\begin{aligned} \omega/kW_s &= 0.5 + i \times 0.34 & (\cos \alpha = 0.5, \omega_1 = \omega_2) \\ \omega/kW_s &= 0.78 + i \times 0.25 & (\cos \alpha = 0.5, \omega_1 = 0.1\omega_2) \\ \omega/kW_s &= 0.22 + i \times 0.25 & (\cos \alpha = 0.5, \omega_1 = 10\omega_2) \end{aligned} \quad (20)$$

When the angle between the spacecraft velocity and the magnetic field is almost equal to 90 deg, the relative speed is less than the IAW phase speed, and the conditions for the two-stream instability are broken in this case. The dispersion relation (15) has two real roots for any values ω_1 and ω_2 :

$$\omega/kW_s = \pm 1 \quad (21)$$

Because of the IAW attenuation, we should not observe the electrostatic noise during the time interval $t \approx 5$ min that is needed to change the angle Θ from 85 to 95 deg (Fig. 8). However, fluctuations

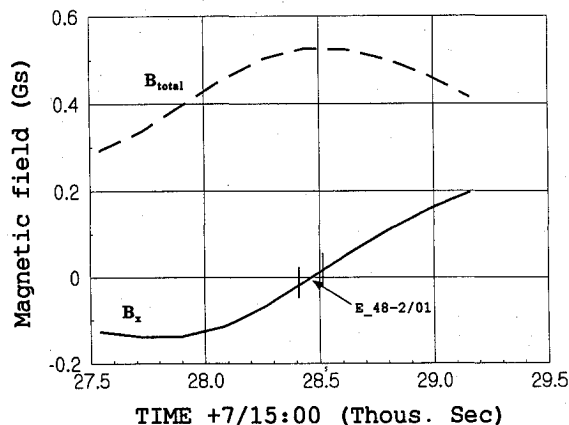


Fig. 8 Magnetic field strength vs time started at MET 7/15:00.

were observed even during the dwell recorded for $V_s \perp B$ (Fig. 4). Such a situation was discussed by Pickett et al.,⁶ and they suggested that a modified two-stream instability (MTSI) could explain the observational data obtained in their experiment for the wake of the Shuttle for $V_s \perp B$. MTSI generates fluctuations with frequencies near the lower hybrid resonance frequency (few kilohertz), and some nonlinear processes should be considered to explain the observed spectrum that has significant amplitudes at frequencies as low as a few hertz.

If we compare our LP data obtained for $B_x = 0$ (Fig. 4) with data obtained for $B_x \leq |B|$ (Figs. 3 and 5), we may suggest that the nature of the turbulence is the same in all three cases because the shape of signals and their spectra is essentially identical. One of the

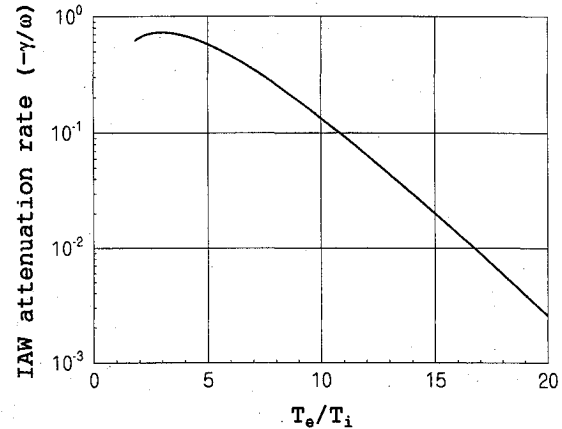


Fig. 9 IAW attenuation rate vs the ratio of electron and ion temperatures.

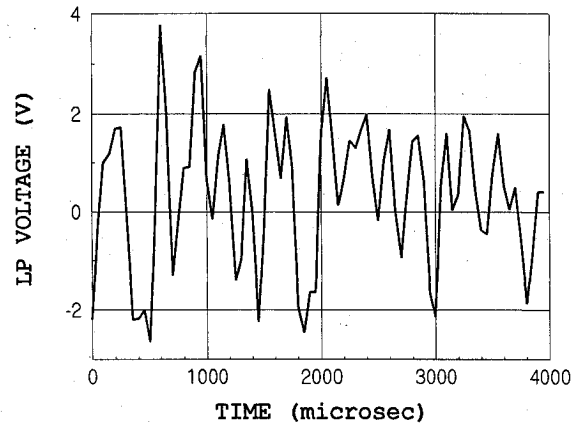


Fig. 10a LP output voltage fluctuations measured during the dwell in RAM conditions when arcing occurred (MET 7/17:21). This plot demonstrates the large amplitude caused by arcing.

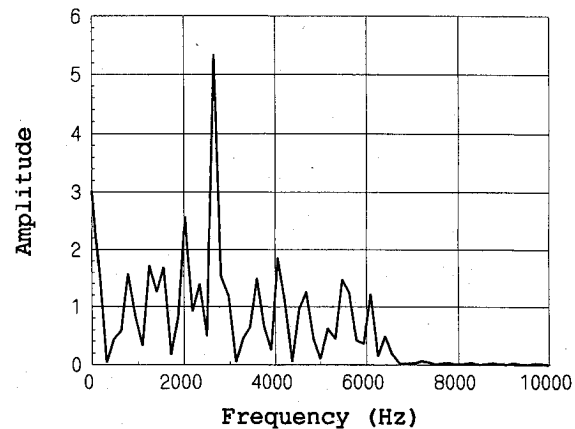


Fig. 10b Spectrum of signal shown in Fig. 10a.

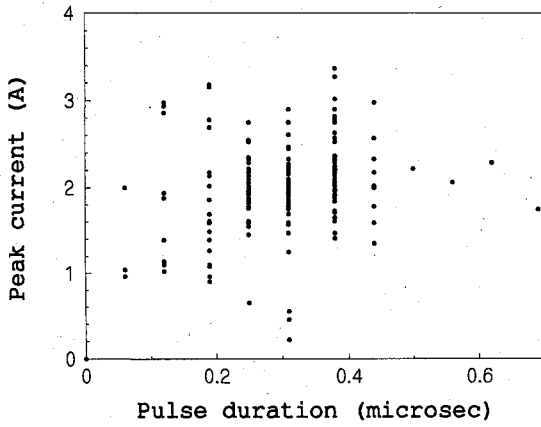


Fig. 11 Data from experiment 60-1/01. The bias voltage $V = -400$ V, and 181 arcs were registered.

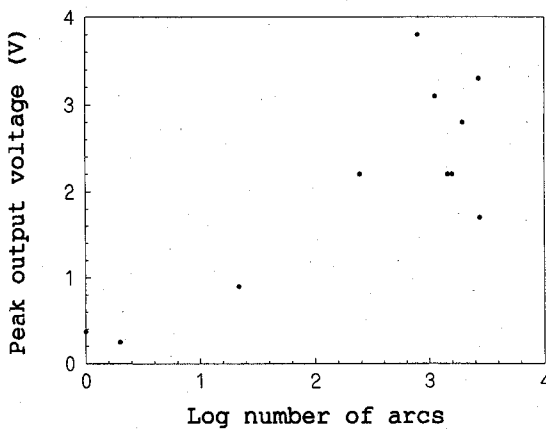


Fig. 12 LP peak voltage vs the number of arcs per one experiment. Twelve dwells are used to draw this chart. No correlations were found between the peak voltage and the distance of the LP from biased solar cell samples.

possibilities to explain the IAW instability is the gradient instability caused by electron and ion number density gradients with a scale $a = [(1/n_i) \times (dn_i/dR)]^{-1} \approx 5$ m [see Eq. (5)]. The dispersion relation can be written in the following form¹⁷:

$$\frac{1}{\Lambda_e^2} + k^2 - \frac{\omega_i^2}{\omega^2} \times k^2 \times \left(1 + \frac{1}{i \cdot k \cdot n_i} \times \frac{dn_i}{dR} \times \sin \varphi \right) = 0 \quad (22)$$

Taking into account that the Debye length is much smaller than the wavelength, we can represent the increment of instability in the following form:

$$\frac{\gamma}{\omega} = \frac{1}{2} \left| \frac{1}{k \cdot n_i} \times \frac{dn_i}{dR} \right| \quad (23)$$

where ω obeys Eq. (21).

It should be noted that Eq. (23) is valid when the angle between the wave vector k and the magnetic field B is not close to zero, but $(k_y/k_z) < 1$, and $(k_x/k_z) < 1$ (k_y is the projection of the wave vector on the direction that is perpendicular to both vectors B and $\text{grad } n_i$). The ratio (23) can be easily estimated for the considered frequency range: $\gamma/\omega = 0.005-0.1$. The attenuation rate of IAW depends on the ratio of the electron temperature to the ion temperature¹⁸ (Fig. 9). The electron temperature is measured for each dwell, and we can use these data for further calculations.

We can estimate the ion temperature by hypothesizing that the main ion component of the plasma is water ions generated by a charge exchange process. Thus we can assume that $T_i < 300$ K. Moreover, the IAW attenuation rate depends on the angle between the wave vector and the magnetic field¹² (Fig. 6). If we compare the attenuation rates mentioned above with increment (23), we see that there is enough room for an instability of IAW even in RAM conditions with $V_s \perp B$ if $(T_e/T_i) \geq 10$.

Influence of Arcing

As was mentioned above, HFT data were also obtained during the experiments when arcs occurred. First, there is a significant difference in amplitudes between signals with arcing and without them (Fig. 10). For this one particular dwell, the amplitude of current fluctuations is as large as $2 \mu\text{A}$.

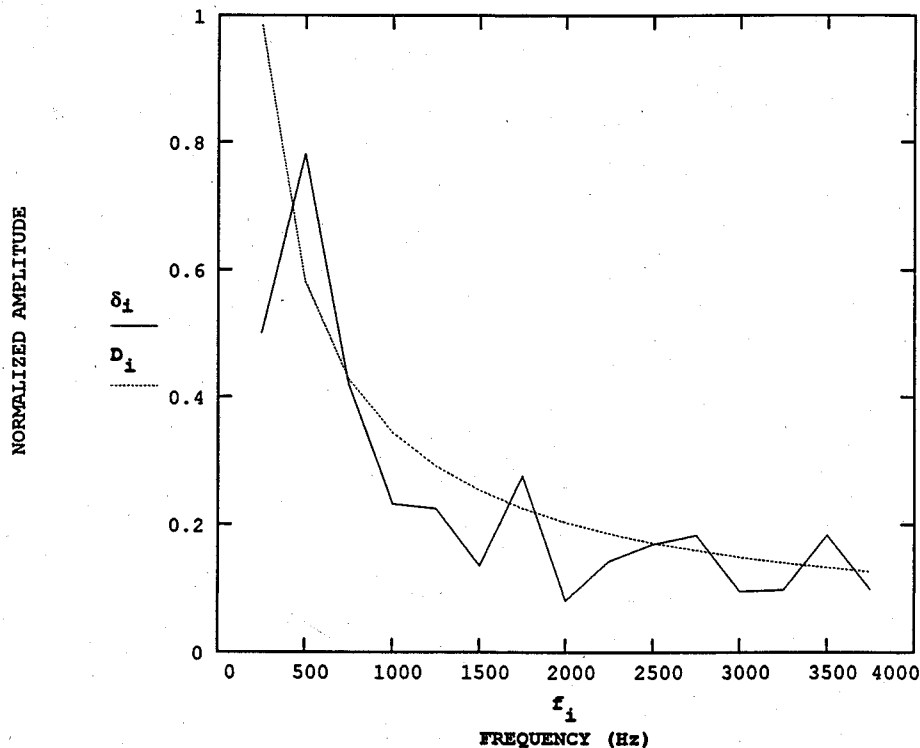


Fig. 13 Average spectrum that was built by using data from twelve dwells without arcing. The best fit approximation $D \propto f^{0.76 \pm 0.2}$ is in good agreement with theoretical predictions.

The number of arcs, the maximum current for each arc, and the duration of the arc were measured by a special counter. One example of data obtained during experiment E_60-1/01 is shown in Fig. 11. There is a strong correlation between the number of arcs observed in an experiment and the amplitude of fluctuations (Fig. 12). These facts show that there is an influence of arcs on the HFT data. We believe that the large amplitude of LP current is caused by rapid changes in the spacecraft potential resulting from arcing. When arcing occurs, the difference of potentials between the Shuttle and the surrounding plasma changes $\Delta V \approx I_m \Delta / C \approx 2-3$ V for the moment of each arc. To obtain the last result, we used the measurements of arc peak current and the duration of each arc (Fig. 11) and an estimate for the capacitance of the Shuttle.¹⁹ Because the duration of each arc is equal to 0.1–0.5 μ s, the moments of arcing are distributed randomly inside the time interval τ_{exp} , the relaxation time for the potential of the Shuttle is less than 50 μ s,¹⁹ and measured value of LP current can be estimated as

$$\Delta I_{\text{max}} = \frac{N_{\text{arc}}}{\tau_{\text{exp}}} \cdot \tau_{\text{dwell}} \cdot \left(\frac{\partial I_{\text{sat}}}{\partial V} \right) \cdot \Delta V \quad (24)$$

For example, during one experiment, $N_{\text{arc}} = 1500$, the duration of the experiment $\tau_{\text{exp}} = 60$ s, and $\tau_{\text{dwell}} = 4$ ms. The value of the expression in the parentheses can be obtained from appropriate sweep data.¹⁰ The result of the calculation, $\Delta I_{\text{max}} \approx 2 \mu$ A, is in agreement with the measurements.

According to theoretical considerations, the spectrum of fluctuations in the plasma should have the following form¹²:

$$D(f) = (A/f) \cdot F(f/f_c) \quad (25)$$

where $A = \text{const}$ and $F(f)$ is a slow function of frequency.

In reality, we obtained $D(f) \propto f^{-0.76 \pm 0.2}$ for the average spectrum without arcing, in agreement with expectations (Fig. 13). We see from the present work that fluctuations with a broad spectrum are developed in the plasma surrounding the shuttle.

Conclusions

During the SAMPIE, fluctuations in the electron number density were observed in RAM conditions. The amplitudes of these fluctuations were as large as 10^{-3} – 10^{-4} from the background density at frequencies $f = 250$ – 6500 Hz. The measurements of the Earth's magnetic field allow us to show that this frequency range is inside the interval $F_i < f < F_{LH}$; thus, we suggest that IAW were observed. An additional argument in favor of the hypothesis of IAW is the inequality between ion and electron temperatures. Measurements have determined that the electron temperature varied from $0.1 \leq T_e \leq 0.3$ eV (Ref. 10). The ion temperature should be substantially lower: $T_i < 0.03$ eV (Ref. 7).

These facts allow us to adopt the basic model of the gas layer around the shuttle. Two kinds of instabilities were suggested for explanation of the origin of IAW: the two-stream instability that works when the angle between the spacecraft velocity and the magnetic field is not too close to a right angle, and the gradient instability that works for situations when the magnetic field and velocity of the shuttle are perpendicular to each other. Note that the last instability is weaker than the first one, and we could observe the transition between the two regimes if the dwell would last for at least several

minutes. More measurements need to be done, particularly for the frequency range 20–100,000 Hz, to allow an understanding of the nature of the observed turbulence.

Acknowledgments

This work was performed while B. V. Wayner held a National Research Council–NASA Lewis Research Center Research Associateship. We thank W. Mackey for useful remarks.

References

- ¹Ferguson, D. C., and Hillard, G. B., "Preliminary Results from the Flight of the Solar Array Module Plasma Interactions Experiment (SAMPIE)," *Proceedings of the XIIIth Space Photovoltaic Research and Technology Conference*, NASA CP-3278, 1994, pp. 247–251.
- ²Wayner, B. V., and Ferguson, D. C., "Electrostatic Noise in the Plasma Environment Around the Shuttle," AIAA Paper 95-1944, June 1995.
- ³Siskind, D. E., Raitt, W. J., Banks, P. M., and Williamson, P. R., "Interactions Between the Orbiting Space Shuttle and the Ionosphere," *Planetary and Space Science*, Vol. 32, No. 8, 1984, pp. 881–896.
- ⁴Murphy, G., Pickett, J., D'Angelo, N., and Kurth, W. S., "Measurements of Plasma Parameters in the Vicinity of the Space Shuttle," *Planetary and Space Science*, Vol. 34, No. 10, 1986, pp. 993–1004.
- ⁵Gurnett, D. A., Kurth, W. S., and Steinberg, J. T., "Plasma Wave Turbulence Around the Shuttle: Results from the Spacelab-2 Flight," *Geophysical Research Letters*, Vol. 15, No. 8, 1988, pp. 760–763.
- ⁶Pickett, J. S., D'Angelo, N., and Kurth, W. S., "Plasma Density Fluctuations Observed During Space Shuttle Orbiter Water Releases," *Journal of Geophysical Research*, Vol. 94, No. A9, 1989, pp. 12,081–12,086.
- ⁷Paterson, W. R., and Frank, L. A., "Hot Ion Plasmas from the Cloud of Neutral Gases Surrounding the Space Shuttle," *Journal of Geophysical Research*, Vol. 94, No. A4, 1989, pp. 3721–3727.
- ⁸Kurth, W. S., and Frank, L. A., "Spacelab-2 Plasma Diagnostic Package," *Journal of Spacecraft and Rockets*, Vol. 27, No. 1, 1990, pp. 70–75.
- ⁹Hillard, G. B., and Ferguson, D. C., "Solar Array Module Plasma Interactions Observed During (SAMPIE): Science and Technology Objectives," *Journal of Spacecraft and Rockets*, Vol. 30, No. 4, 1993, pp. 488–494.
- ¹⁰Morton, T. L., Ferguson, D. C., and Hillard, G. B., "Ionospheric Plasma Densities and Temperatures Measured by SAMPIE," AIAA Paper 95-0841, Jan. 1995.
- ¹¹Bozich, R., private communication, LYMA, Cleveland, OH, 1994.
- ¹²Al'pert, Y. L., *Space Plasma*, 1st ed., Vol. 1, Cambridge Univ. Press, Cambridge, MA, 1990.
- ¹³Dean, D. A., Huppi, E. R., Smith, D. R., Nadile, R. M., and Zhou, D. K., "Space Shuttle Observations of Collisionally Excited Outgassed Water Vapor," *Geophysical Research Letters*, Vol. 21, No. 7, 1994, pp. 609–612.
- ¹⁴Zhou, D. K., Pendleton, W. R., Bingham, G. E., Steed, A. J., and Dean, D. A., "Infrared Spectral Measurements (450 – 2500 cm^{-1}) of Shuttle-Induced Optical Contamination," *Geophysical Research Letters*, Vol. 21, No. 7, 1994, pp. 613–616.
- ¹⁵Kaplan, S. A., and Pikel'ner, S. B., *Physics of Interstellar Medium*, 2nd ed., Nauka, Moscow, 1979.
- ¹⁶Akhiezer, A. I., Akhiezer, I. A., Polovin, R. V., Sitenko, A. G., and Stepanov, K. N., *Electrodynamics of Plasma*, 1st ed., Nauka, Moscow, 1974.
- ¹⁷Timofeev, A. V., "Dissipative Instability of a Weakly Ionized Inhomogeneous Plasma in a Uniform External Magnetic Field," *Soviet Physics-Technical Physics*, Vol. 8, No. 8, 1964, pp. 682–685.
- ¹⁸Krall, N. A., and Trivelpiece, A. W., *Principles of Plasma Physics*, 1st ed., McGraw-Hill, New York, 1973.
- ¹⁹Purvis, C. K., Ferguson, D. C., Snyder, D. B., Grien, N. T., Staskus, J. V., and Roche, J. C., "Environmental Interactions Considerations for Space Station and Solar Array Design," NASA Lewis Research Center Internal Rept., 1986, pp. 20, 21.